International Journal of Biochemistry and Cell Biology 116 (2019) 105617

Contents lists available at ScienceDirect

International Journal of Biochemistry and Cell Biology

journal homepage: www.elsevier.com/locate/biocel

Downregulation of Rab23 inhibits proliferation, invasion, and metastasis of human ovarian cancer

Lingling Gao[a,b], Mingjun Zheng[a,b], Qian Guo[a,b], Xin Nie[a,b], Xiao Li[a,b], Yingying Hao[a,b], Juanjuan Liu[a,b], Liancheng Zhu[a,b], Bei Lin[a,b,*]

[a] Department of Obstetrics and Gynecology, Shengjing Hospital Affiliated to China Medical University, Heping District, Shenyang, Liaoning, China
[b] Key Laboratory of Maternal-Fetal Medicine of Liaoning Province, Key Laboratory of Obstetrics and Gynecology of Higher Education of Liaoning Province, Liaoning, China

ARTICLE INFO

Keywords:
Rab23
Ovarian cancer
Proliferation
Invasion
Metastasis

ABSTRACT

Previously, we reported that the expression of human epididymis protein (HE4) was correlated with the expression of *RAB23* in ovarian cancer cells. Rab23 is a member of the Ras-related small GTPase superfamily, which plays a key role in the Sonic Hedgehog (Shh) signaling pathway. However, the function of Rab23 in ovarian cancer remains unclear. In this study, we explored the location and expression of Rab23 in ovarian cancer tissues and cells (CaoV3 and A2780), and further investigated the function and potential mechanism of Rab23 in malignant biological behaviors including the epithelial-mesenchymal transition (EMT) process in ovarian cancer for the first time. Rab23 is highly expressed in ovarian cancer tissues and associated with advanced stage, and shortened overall survival time of ovarian cancer patients. We are the first to report that human epididymis protein (HE4) can regulate the expression of the Rab23 protein, and that knockdown of *RAB23* decreases the proliferation, invasion, and migration abilities as well as inhibits the epithelial-mesenchymal transition (EMT) process in ovarian cancer cells. Furthermore, downregulation of Rab23 significantly inhibited Shh-Gli1 and PI3K-AKT signaling pathways. Collectively, our results indicate that Rab23 plays a critical role in the malignant biological behavior of ovarian cancer and may serve as a potential biomarker and therapeutic target for ovarian cancer.

1. Introduction

Ovarian cancer is one of the most common and deadliest malignant tumors in gynecology, and it is often diagnosed at an advanced stage with extensive metastasis (Siegel et al., 2017). In the past 20 years, the five-year overall survival rate of patients with ovarian cancer, less than 45%, has not significantly improved (Webb and Jordan, 2017). There are no effective therapies for ovarian cancer, and the molecular mechanisms underlying its occurrence and development have not been fully clarified. Therefore, identifying the key mechanisms that influence the occurrence, development, invasion, and metastasis of ovarian cancer at a molecular level will provide potential new therapies to improve the prognosis of ovarian cancer patients.

Rab23 is a member of the Ras-related small GTPase family, which is the biggest subfamily of the Ras superfamily. The *RAB23* gene is located at chromosome 6p12.1-q12, and its mutation can induce open brain syndrome in mice (Guo et al., 2006). Rab23 protein can be found in brain, stomach, breast, testes, ovary, and other tissues, indicating that it is involved in various physio-pathological processes. Mutations in Rab23 can result in some congenital disease, such as Carpenter syndrome and Stevenson-Johnson syndrome. In 1994, Olkkonen et al. isolated the full-length *RAB23* cDNA from mouse brain (Olkkonen et al., 1994). In 2001, Eggenschwiler found that Rab23 was an important negative regulator of the Sonic Hedgehog signaling pathway, suggesting that Rab23 has a tumor-suppressing role (Eggenschwiler et al., 2001). Chi observed that Rab23 negatively regulated Gli activity in a Su (Fu)-dependent way (Chi et al., 2012). In recent years, many studies have shown that Rab23 can promote tumor development. So far there is only one study of Rab23 in ovarian cancer, which demonstrated that Rab23 could facilitate the resistance of ovarian cancer cells to platinum drugs via the Shh-Gli1-ABCG signaling pathway (Zhang et al., 2018). However, the role of Rab23 in the occurrence and development of ovarian cancer and its effects on malignant behaviors in ovarian cancer cells have not been investigated. Using gene chip analysis, our team found that Rab23 expression was associated with the expression of HE4 in ovarian cancer cells (Zhu et al., 2016). In order to further verify and

* Corresponding author at: Department of Obstetrics and Gynecology, Shengjing Hospital Affiliated to China Medical University, No. 36 Sanhao Street, Heping District, Shenyang, 110004, Liaoning, China.
E-mail address: linbei88@hotmail.com (B. Lin).

https://doi.org/10.1016/j.biocel.2019.105617
Received 28 March 2019; Received in revised form 30 August 2019; Accepted 18 September 2019
Available online 21 September 2019

explore the correlation of Rab23 with the occurrence and development of ovarian cancer, the expression and clinical significance of Rab23 in ovarian cancer were detected by clinical samples. Specifically, we validated and explored the potential interaction between HE4 and Rab23. The current study is primarily aimed at exploring the influence of Rab23 on the malignant behavior of ovarian cancer cells and potential signaling pathways, which will provide new directions for the early diagnosis, and clinical treatment of ovarian cancer.

2. Materials and methods

2.1. Patients and tissue samples

The study was approved by the Research Ethics Board at Shengjing Hospital of China Medical University. A total of 162 paraffin-embedded surgical pathological specimens were collected from the Department of Obstetrics and Gynecology in Shengjing Hospital of China Medical University from 2008 to 2014. The pathological diagnosis for each tissue section was confirmed by the pathologists. The 162 specimens consisted of 119 malignant epithelial ovarian tumors (malignant group), 10 borderline epithelial ovarian tumors (borderline group), 13 benign epithelial ovarian tumors (benign group), and 20 normal ovarian tissues (normal group). The normal ovarian tissues were collected from patients with undesired fertility due to cervical cancer operations. The average patient age was 54.44 years (19 to 83) in the ovarian cancer group, 49.40 years (26 to 84) in both the borderline and benign groups, and 44.17 years (36 to 57) in the normal group, there were no statistically significant differences in ages among the various groups ($P > 0.05$). In the malignant group, the pathological types were as follows: 59 serous ovarian cancers, 12 mucinous adenocarcinomas, 21 endometrioid adenocarcinomas, 8 clear cell carcinomas, and 19 cases of poorly differentiated adenocarcinoma. The malignant group consisted of patients with cancer tissues exhibiting well (34), moderate (29), and poor (56) differentiation. Based on the International Federation of Gynecology and Obstetrics (FIGO, 2009), pathological stages were as follows: stages I-II (54 cases), stages III-IV (65 cases). Lymph node metastasis was judged as follows: no metastasis (74 cases), metastasis (23 cases), and no lymphadenectomy (22 cases). All cases were primary ovarian cancer with complete clinical pathological data.

2.2. Immunohistochemistry and immunocytochemical staining

Specimens (5 μm continuous sections) were fixed with 10% formalin, embedded in paraffin. Rab23 expression was detected by immunohistochemical streptavidin peroxidase staining (Ultrasensitive ™ SP (Mouse/Rabbit) IHC Kit, Maixin, China) according to the manufacturer's instructions. Liver cancer tissues served as positive controls; phosphate buffered saline (PBS) was used instead of primary antibody for the negative controls. The working concentrations of primary antibodies against Rab23 used were 1:75 (Proteintech, Wuhan, China, Cat# 11101-1-AP).

For immunocytochemistry, cells in the logarithmic growth phase were digested by 0.25% trypsin and adherently grown as a single layer. The adherent cells were washed three times with cold PBS and then fixed with 4% paraformaldehyde at room temperature for 20 min. The following steps were the same as immunohistochemistry.

The presence of buffy granules in the cell membrane and cytoplasm was defined as positive. The staining intensity was scored as 0 (no pigmentation), 1 (yellow), 2 (brown-yellow), and 3 (brown). The percentage of stained cells in the whole section was scored as follows: 0 score, < 5%; 1 score, 6%–25%; 2 scores, 26–50%; 3 scores, 51–75%; 4 scores, > 75%. The final score was obtained by multiplying the staining intensity score by the percentage of stained cells score: 0–2 scores, (-); 3–4 scores, (+); 5–8 scores, (++); 9–12 scores, (+++). Two senior pathologists scored the sections independently to control for error. If there was a contradiction or dispute, a third pathologist evaluated the sample.

2.3. Cell culture and transfection

The ovarian cancer cell lines CaoV3 and A2780 from the Institute of Biochemistry and Cell Biology, Chinese Academy of Sciences (Shanghai, China). were cultured in RPMI 1640 containing 10% fetal bovine serum (FBS) (Thermo Fisher Scientific, Waltham, MA, USA) at 37 °C, 5% CO_2, and saturated humidity. The stably low expression HE4 ovarian cancer cell line (CaoV3-HE4-L) constructed by lentivirus were the same culture conditions with puromycin (Zhuang et al., 2014b). The day before transfection, exponentially growing cells were seeded into 6-well plates. When the cells had grown to 50% to 70% confluence, they were transfected with various RNAi molecules using a Lipofectamine 3000 Transfection Kit (Invitrogen, Carlsbad, CA) according to the manufacturer's instructions. Interference effect were analyzed after transfection 48 h. The Rab23 RNAi sequences were 5′- GGAGGAAUUUGAU GCAAUUTT-3′(forward), and 5′-AAUUGCAUCAAAUUC CUCCTT-3′(reverse); the negative control sequences were 5′-UUCUCCGAACGUG UCACGUTT-3′(forward) and 5′-ACGUGACACGUUCGGAGAATT-3′ (reverse).

2.4. Western blot

Cells were collected and washed with pre-cooled 1 × PBS three times at 1500 rpm for 10 min at 4 °C. Ice-cold RIPA buffer was added to the cell pellet, and lysis was allowed to proceed for 30 min at 4 °C. After centrifugation at 12,000 rpm for 30 min at 4 °C, the protein concentration was determined with the BCA method. SDS-PAGE loading buffer (reducing 5×) (CWVBIO, China) was added to the samples for 5 min at 100 °C; denatured protein were separated by 10% sodium dodecyl sulfate-polyacrylamide gel electrophoresis. The proteins were transferred to polyvinylidene fluoride membrane (PVDF) (Millipore, USA) and blocked with 5% skim milk or BSA for 2 h at room temperature. The following primary antibodies were incubated overnight at 4 °C respectively: anti-Rab23 (Proteintech, Wuhan, China, Cat# 11101-1-AP), anti-E-Cadherin (Proteintech, Wuhan, China, Cat# 20874-1-AP), anti-MMP2 (Proteintech, Wuhan, China, Cat# 10373-2-AP,) and anti-MMP9 (Proteintech, Wuhan, China, Cat# 10375-2-AP); anti-N-Cadherin (Proteintech, Wuhan, China, Cat# 22018-1-AP); anti-PI3K (Cell Signaling Technology, Inc., Cat# 4292S), anti-*p*-PI3K (Cell Signaling Technology, Inc., Cat# 4228S), AKT (Cell Signaling Technology, Inc., Cat# 4691S), anti-*p*-AKT (Cell Signaling Technology, Inc., Cat# 4060S); anti-Shh (Cell Signaling Technology, Inc., Cat# 2207S); anti-Gli1 (Cell Signaling Technology, Inc., Cat# 2643S) and anti-GAPDH (ZSGB-BIO, China,). After washing with 1 × TBST for 10 min three times, secondary antibodies (ZSGB-BIO, China, 1:5000) were incubated with the blots at room temperature for 2 h, and then washed as described above. Proteins were visualized using Immobilon® Western chemiluminescent HRP Substrate (Millipore, Billerica, MA, USA). The experiments were repeated three times.

2.5. Cell proliferation assay

Cells in exponential growth phase were digested with 0.25% trypsin to obtain single cell suspensions and then seeded in 96-well cell culture plates (2,000/well). Optical density (OD) was evaluated at 0, 24, 48, 72, and 96 h. The MTT solution (20 μl; 5 mg/ml; Solarbio, Beijing, China) was added to each well, and incubated at 37 °C for 4 h. After the removal of culture medium, 150 μl DMSO was added. After shaking for 10 min, the OD was measured at 490 nm. There are six parallel wells in each group. The experiment was repeated three times.

2.6. Cell scratch assay

Single cell suspensions were prepared from cells in exponential

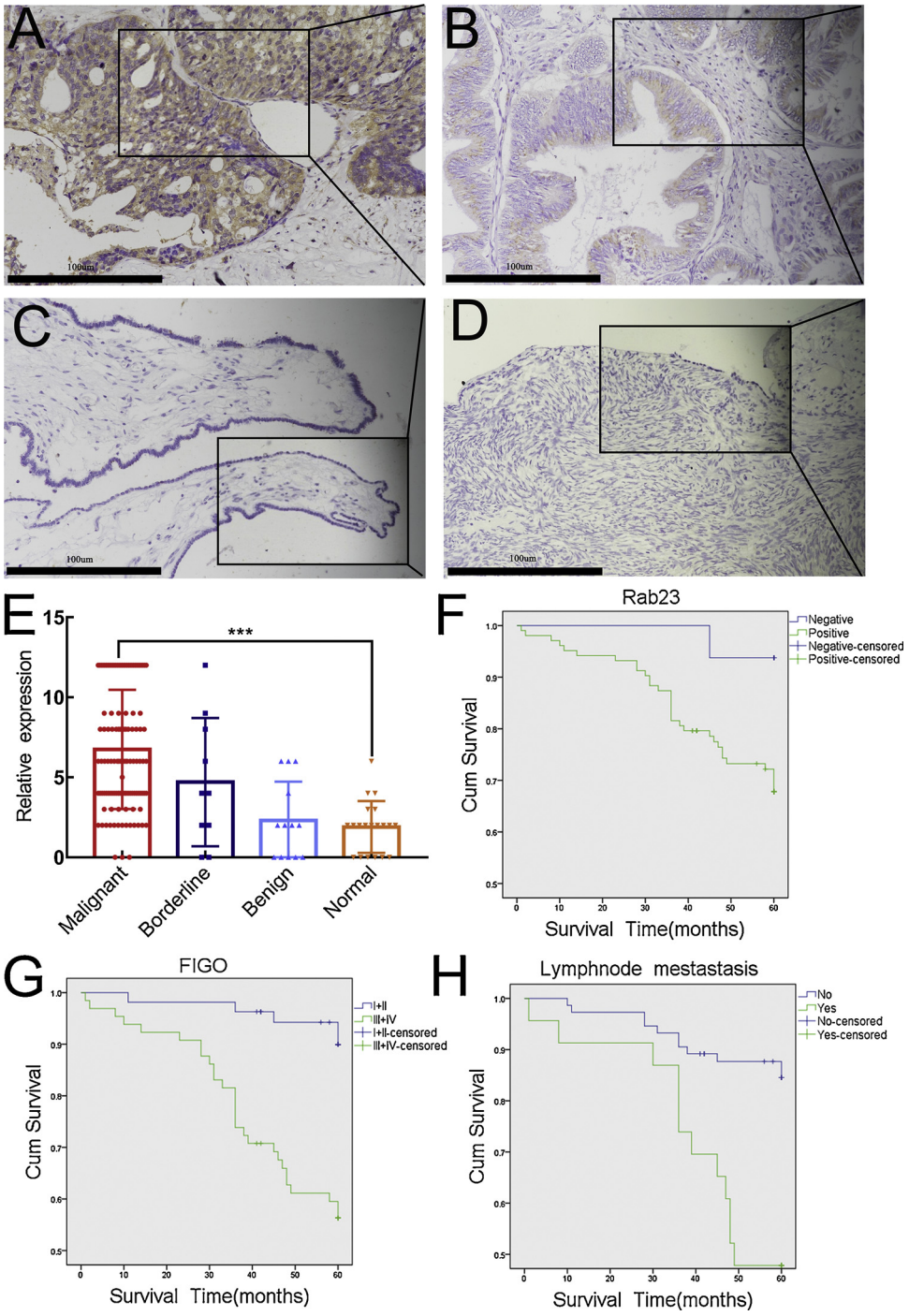

Fig. 1. Expression and prognostic significance of Rab23 in patients with ovarian cancer. (A–D) Representative immunohistochemical staining images for Rab23 expression in different ovarian tissues (SP × 200, central SP × 400). (A) Malignant ovarian tumor. (B) Borderline ovarian tumor. (C) Benign ovarian tumor. (D) Normal ovarian tissue. (E) Rab23 expression in malignant ovarian tumor compared with normal group (***$P < 0.001$). (F–H) Kaplan-Meier analysis of the prognosis of ovarian cancer. Relationship between prognosis and high Rab23 expression (F), FIGO stage (G), lymph node metastasis (H). Scale bar: 100 μm. SP: scaled pixels.

growth phase, and seeded in 6-well plates. After the cells reached 90% confluence, the plate was gently scratched in a straight line with a 200 μL pipette tip and then washed three times with PBS. The remaining cells were cultured in medium without serum for 24 h. The scratch width was measured at 0 and 24 h under the microscope. Experiments were repeated three times.

2.7. Transwell assay

Matrigel was thawed overnight at 4 °C and diluted with ice-cold serum-free culture medium at a ratio of 1:8. The upper well of the Transwell chamber was layered with Matrigel and then incubated at 37 °C for 4 h until the Matrigel solidified. Cells (2×10^5) in serum-free medium (200 μl) were seeded in the upper chamber, then 500 μl of complete medium was added to the lower chamber. After incubation at 37 °C for 48 h, the Transwell chamber was washed with PBS three times, then cells were fixed with 4% paraformaldehyde for 30 min. After staining with crystal violet for 30 min, cells in the upper chamber were gently removed with cotton swabs. Five fields randomly selected under the microscope were calculated. The experiment was repeated

Table 1
Expression of Rab23 in different ovarian tissues.

Groups	Cases	Low		High		Positive Rate (%)	High expression Rate (%)
		−	+	++	+++		
Malignant	119	16	32	34	37	86.6% [a, b]	59.7% [c, d]
Borderline	10	4	2	2	2	60.0% [e, f]	40.0% [g]
Benign	13	9	1	3	0	30.8%	23.1%
Normal	20	15	4	1	0	25.0%	5.0%

Note: [a] malignant ovarian tumors versus benign ovarian tumors, $P < 0.001$; [b] malignant ovarian tumors versus normal ovarian tissue, $P < 0.001$; [c] malignant ovarian tumors versus benign ovarian tumors, $P = 0.0014$; [d] malignant ovarian tumors versus normal ovarian tissue, $P < 0.001$; [e] borderline ovarian tumors versus benign ovarian tumors, $P = 0.019$; [f] borderline ovarian tumors versus normal ovarian tissue, $P = 0.018$; [g] borderline ovarian tumors versus benign ovarian tumors or normal ovarian tissue, $P = 0.015$.

three times.

2.8. Gene set enrichment analysis, GSEA

GSEA 3.0 software was used for analysis. The dataset for c2.cp.kegg.v6.1.symbols.gmt was downloaded from the MsigDB database on the GSEA website. Enrichment analysis was performed on the expression spectrum data and attribute files after high and low grouping using the default-weighted enrichment analysis method. The random assortment frequency was set as 1000.

2.9. Function and pathway enrichment analysis

The proteins interacting with Rab23 were identified from the GCBI protein database, then the corresponding genes were subject to Gene Ontology (GO) functional analysis via the Bioinformatics Resources (http: //david.abcc.ncifcrf.gov/). The significance of these enriched genes identified using the Kyoto Encyclopedia of Genes and Genomes (KEGG) pathway was calculated by hypergeometric testing using the formula

$$P = 1 - \sum_{k=0}^{m} \frac{\binom{n}{k}\binom{N-n}{M-k}}{\binom{N}{M}} \quad P = 1 - \sum_{k=0}^{m} \frac{\binom{n}{k}\binom{N-n}{M-k}}{\binom{N}{M}}$$

where N is the number of genes in the whole genome, M represents the number of genes in the whole genome that were annotated to a given pathway, n is the number of genes in the interaction network, and m is the number of genes annotated to a given pathway.

2.10. Construction and module screening of the protein-protein interaction network

The protein-protein interaction (PPI) network was constructed using the STRING (http://string.embl.de/) online tool. The visualization plot was generated using Cytoscape software with a confidence score of ≥ 0.1 defined as the cutoff. The core modules of the PPI network were screened using Molecular Complex Detection (MCODE) with the following parameters: degree threshold = 2, node threshold = 0.2, k-core = 2, and maximum depth = 100. The genes in the core modules were subject to KEGG and GO analyses.

2.11. Statistical analysis

All data were analyzed using SPSS 21.0 statistical software (IBM Corporation, Armonk, NY, USA), graphs were generated with Graphpad Prism 7.0 Software (GraphPad Software, Inc., San Diego, CA). The results are presented as the mean ± standard deviation (SD). Student's *t*-test, Chi-squared test, and one-way ANOVA were employed where appropriate. Kaplan-Meier and log-rank were used for survival analysis. A bilateral $P < 0.05$ indicated statistical significance, *, $P < 0.05$; **, $P < 0.01$; ***; $P < 0.001$.

3. Results

3.1. Rab23 expression in different ovarian tissues

Rab23 was present in the cytoplasm and cell membrane but rarely in the nucleus (Fig. 1A-D). The positive and high positive expression rates in the ovarian cancer group were 86.6% (103/119) and 59.7% (71/119), respectively, which were significantly higher than those in the benign group (30.8% [4/13] and 23.1% [3/13]; both $P < 0.05$) or normal group (25% [5/20] and 5% [1/20]; both $P < 0.001$). In the borderline group, the positive rate of Rab23 was 60% (6/10), which was greater than that of the benign (30.8% [4/13]) or normal groups (25% [5/20]) ($P < 0.05$). The high positive rate of Rab23 in borderline group was 40% (4/10), which was also higher than that of the normal group (5% [1/20]; $P < 0.05$) (Fig. 1E and Table 1). The rate of Rab23 positive expression in the benign group was higher than that in normal group, but the differences were not statistically significant.

3.2. Correlation between Rab23 expression and clinical pathological parameters of ovarian cancer

A total of 119 ovarian cancer specimens were evaluated in this study. The positive rate of Rab23 expression in cancer tissues in stages III-IV was 96.9% (63/65), which was significantly higher than tissues in stages I-II (74.1% [40/54]; $P < 0.05$). The ovarian cancer group was further divided into high (++, +++) and low Rab23 expression groups (-, +). In stages III-IV, the high positive rate of Rab23 expression was 67.7% (44/65), which was significantly higher than in stages I-II (50% [27/54]; $P < 0.05$). There was no statistical difference between Rab23 expression and age, pathological type, differentiation degree, and lymph node metastasis of patients at diagnosis (Supplementary Table 1).

3.3. Positive expression of Rab23 was associated with poor prognosis in ovarian cancer patients

Ovarian cancer patients were followed through December 30, 2017. Kaplan-Meier analysis showed that positive expression of Rab23 was significantly associated with a shortened overall survival ($P < 0.05$). The average survival time in the Rab23 positive expression group was 42.20 months, while the average survival time in the negative expression group was 59.06 months. In addition, FIGO stage (I-II *versus* III-IV) and lymph node metastasis (yes *versus* no) were all correlated with poor prognosis ($P < 0.05$) (Fig. 1F–H and Supplementary Table 2).

3.4. Correlation between expression of Rab23 and HE4

A total of 95 ovarian cancer tissues were evaluated in this study. Correlation analysis showed that there was a positive correlation between the expression of Rab23 and HE4 in ovarian cancer(the Spearman correlation coefficient Rs = 0.336, $P = 0.001$)(Table 2 and Fig. 2A). Univariate linear regression analysis showed that Rab23 and HE4 protein expressions can affect each other (both $P < 0.05$) (Table 3). As was presented in Table 3, FIGO stage was a significant affective factor of HE4 expression ($P = 0.003$). In multivariate linear regression analysis of the Rab23 expression score (from 0 to 12), we found that HE4 expression was the independent factor of Rab23 expression, and Rab23 was an independent factor of HE4 expression ($P = 0.001$ and $P = 0.004$) (Table 3). In order to further detect the relationship between them, we searched Rab23 and HE4-related genes in the cBioPortal database and constructed a PPI network using String (Fig. 2B), the results showed that there was an indirect relationship

Table 2
The correlation between Rab23 and HE4 expression in ovarian cancer (the Spearman correlation coefficient Rs = 0.336, P = 0.001).

Rab23	HE4				case
	–	+	++	+++	
–	5	5	1	3	14
+	3	7	5	10	25
++	4	3	6	17	30
+++	1	3	6	16	26
case	13	18	18	46	95

between Rab23 and HE4. After downregulation of *RAB23*, there was no significant change in HE4 expression level (Fig. 2C). However, protein levels of Rab23 significantly decreased after downregulation of HE4 expression in Caov3-HE4-L cells (Fig. 2D).

3.5. Function and pathway enrichment analysis of Rab23 protein

Function and pathway enrichment analysis were performed on the related genes in the PPI network via the DAVID database. The top 20 GO terms and pathways were visualized using the "ggplot2.R" software package. The genes participated in several biological processes, such as histone deacetylation and negative regulation of apoptosis (Fig. 3A).

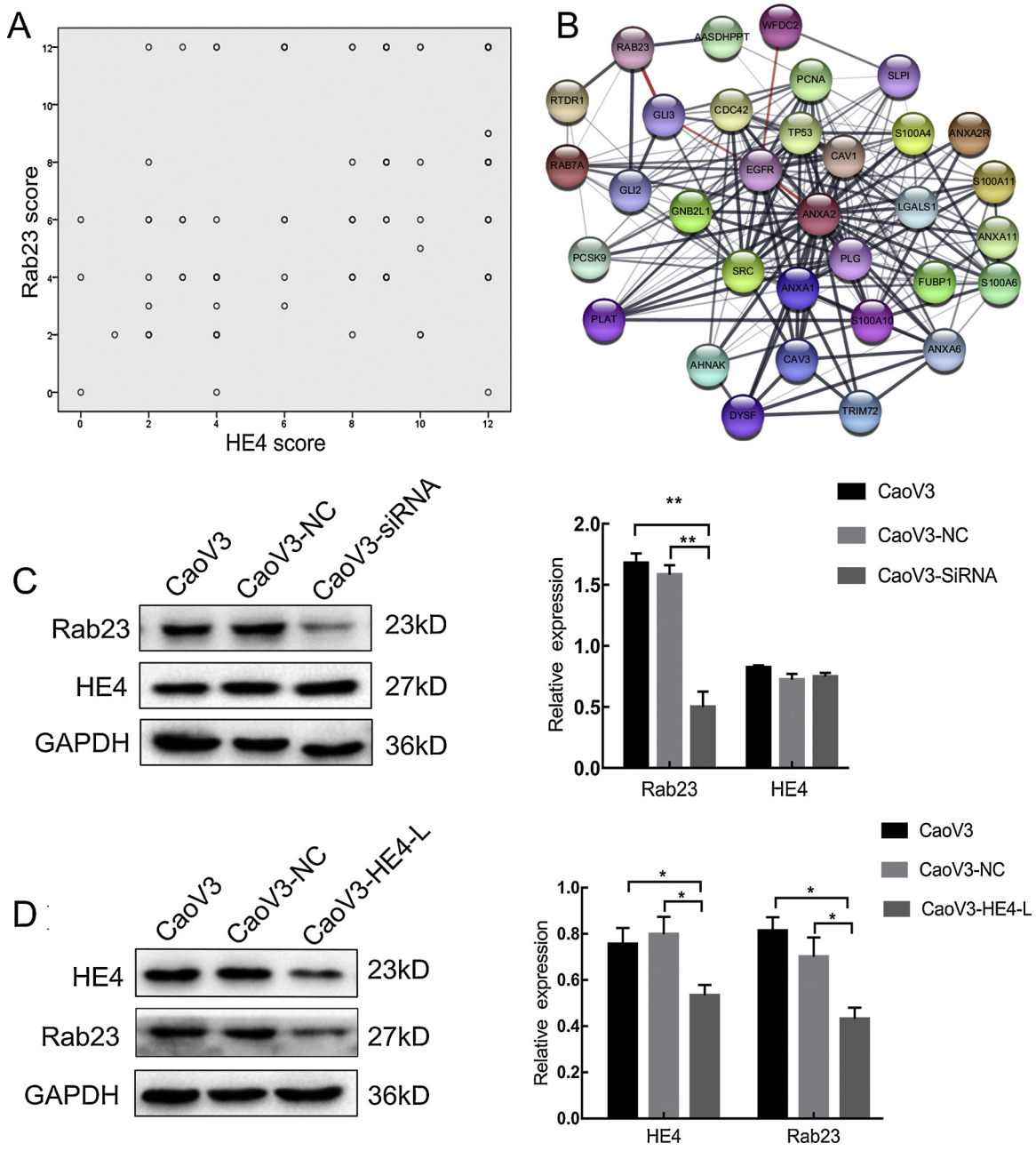

Fig. 2. Regulatory relationship between Rab23 and HE4. (A) The correlation between Rab23 and HE4 expression with Scatter plot. (B) Prediction map of Rab23 and HE4 PPI network : A node indicates a protein and the edge between two nodes represents the interaction between two connected proteins. The different color edges are different interaction evidence sources. If more nodes are connected, it indicates a more important position of the protein in the network. (C) Changes in HE4 protein levels in CaoV3 cell after downregulation of Rab23 expression detected by Western blot. (D) Changes in Rab23 expression in CaoV3-HE4-L cells by Western blot. *$P < 0.05$; **$P < 0.001$. Rab23, member RAS oncogene family; HE4: Human epididymis protein 4; CaoV3-NC: negative control group; CaoV3-siRNA: down-regulation of Rab23 expression in CaoV3; CaoV3-HE4-L: downregulation of HE4 expression in CaoV3 constructed by lentivirus.

Table 3
Linear regression analysis of Rab23 and HE4 expression.

	Rab23 score				HE4 score			
	Univariate		Multivariate		Univariate		Multivariate	
	β	*P*	β	*P*	β	*P*	β	*P*
HE4 score	0.332	**0.001**	0.327	**0.001**#				
Rab23 score					0.417	**0.001**	0.287	**0.004***
Age at diagnosis	0.078	**0.022**	0.076	**0.019**	0.007	0.849		
FIGO stage	0.643	0.111			1.192	**0.003**		
Differentiation	0.756	0.170			0.997	0.071		
Lymphatic metastasis	0.281	0.785			0.289	0.548		

Note: Significant *P* values are indicated in bold; #represents the multivariate regression analysis when Rab23 score was dependent variate, including HE4 score, age at diagnosis as independent variables; *represents the multivariate regression analysis when HE4 score was dependent variate, including Rab23 score and FIGO stage as independent variables.

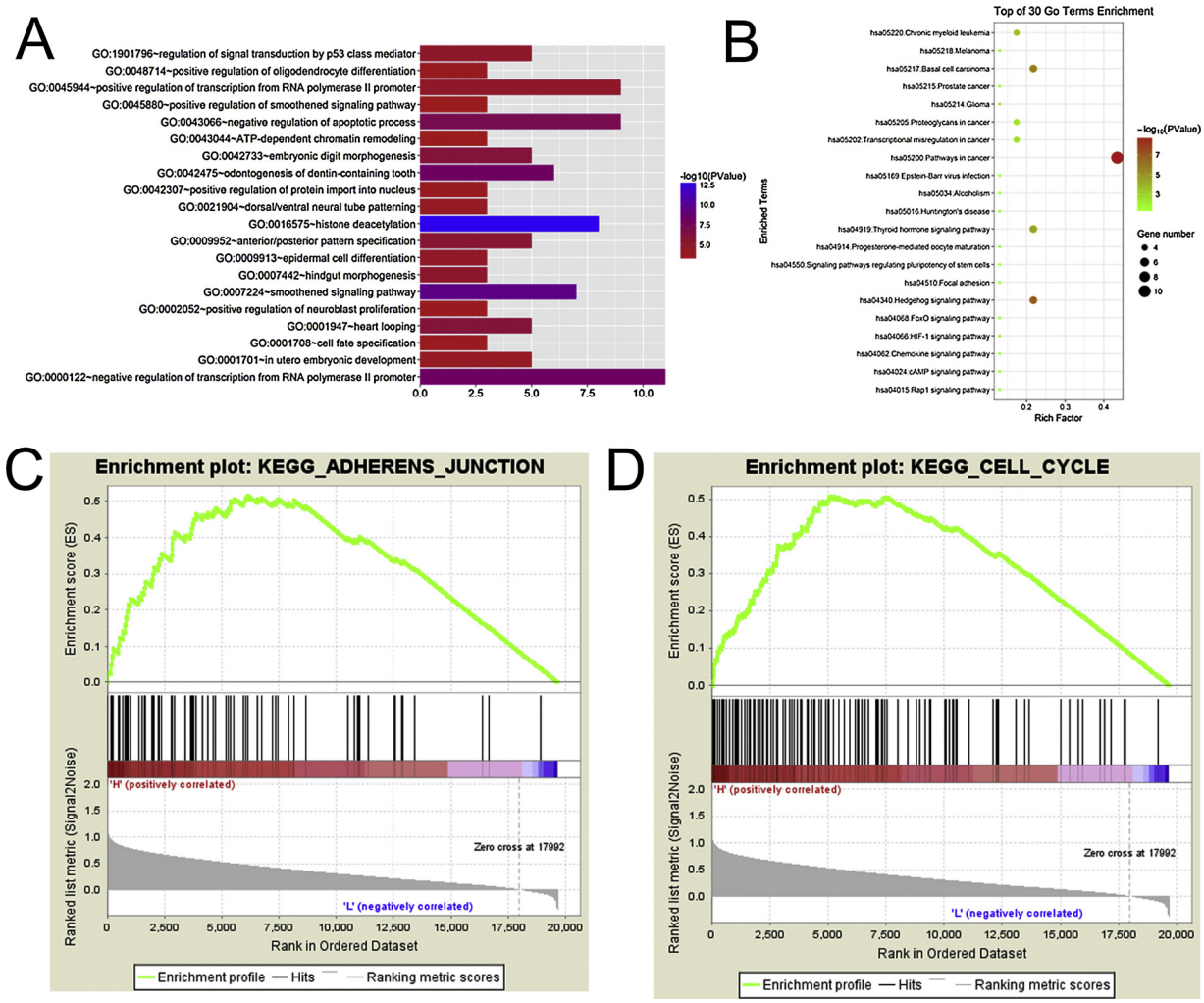

Fig. 3. Function and pathway enrichment analysis of Rab23 protein. (A) Function enrichment analysis histogram of the PPI network. The vertical and horizontal axes represent the name of the pathway or function and the number of enriched genes, respectively. The color indicates the statistical significance with blue corresponding to a smaller *P*-value. (B) Pathway bubble diagram showing the enrichment of genes in the PPI network. The vertical and horizontal indicate the pathway or function name and the percentage in the whole network, respectively. The bubble size shows the number of genes in the pathway. The color represents the *P*-value of the enrichment with a darker color indicating the greater significance of the results. (C–D) GSEA analysis of Rab23-reated enrichment gene sets. (C) Adhesive bridging: KEGG_ADHERENS_JUNCTION (P-value = 0.000; FDR = 0.033; Enrichment score = 0.516). (D) Cell cycle: KEGG_CELL_CYCLE (P-value = 0.000; FDR = 0.039; Enrichment score = 0.508. KEGG: Kyoto Encyclopedia of Genes and Genomes; FDR: False Discovery Rate; GSEA: Gene set enrichment analysis.

Rab23 was mainly enriched in the Hedgehog signaling pathway and signaling pathways associated with cancer (Fig. 3B). GSEA indicated that the samples with high Rab23 expression were enriched in the gene sets of the cell cycle and adhesive bridging (Fig. 3C-D).

3.6. Proliferation, invasion, and migration of ovarian cancer cells weakened after Rab23 downregulation

To further explore the effects of Rab23 on the proliferation,

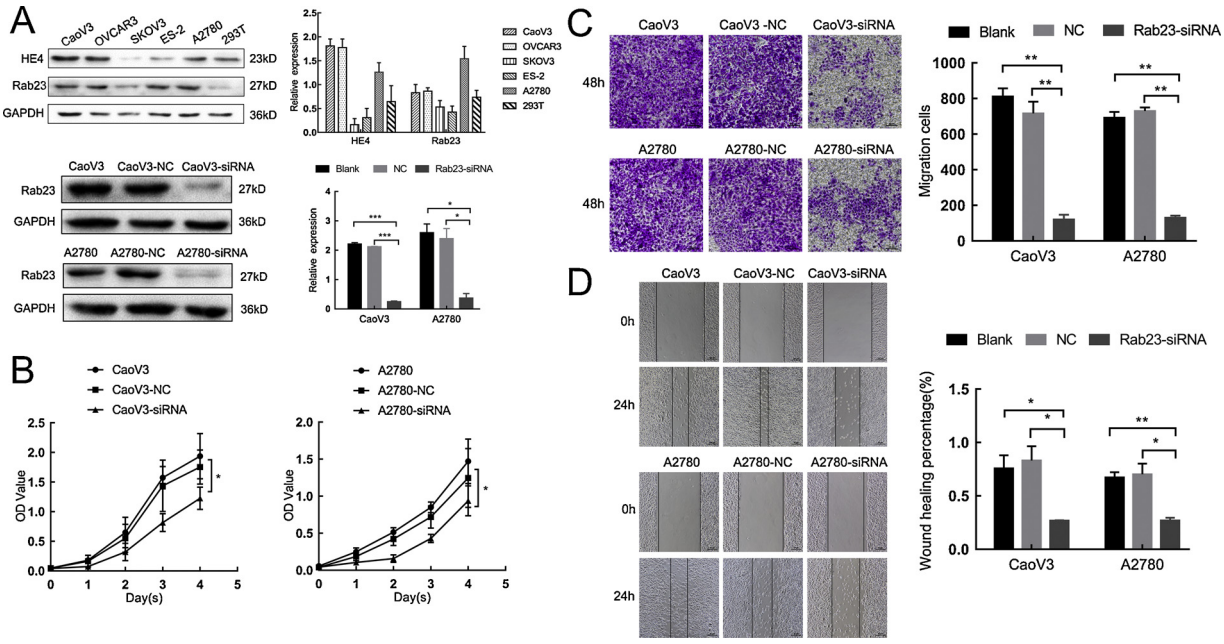

Fig. 4. Effects of Rab23 downregulation on the biological behaviors in CaoV3 and A2780. (A) Rab23 expression in different ovarian cancer cells and 293 T cells and downregulation of Rab23 expression in CaoV3 and A2780 detected by western blot. (B) Changes in proliferation of CaoV3 and A2780 cells after Rab23 downregulation measured by MTT assay. (C) Changes in cell invasion of CaoV3 and A2780 cells after Rab23 decreased using the Transwell assay. Scale bar: 10 μm. (D) Changes in the migration of CaoV3 and A2780 cells after Rab23 downregulation measured by scratch test. Scale bar: 100 μm. Data are represented as the mean ± SD of three replicates. *$P < 0.05$; **$P < 0.01$; **$P < 0.001$. MTT: 3-(4,5-dimethyl-2-thiazolyl)- 2,5-diphenyl-2-H-tetrazolium bromide, Thiazolyl Blue Tetrazolium Bromide; Blank: untreated blank control group; NC: negative control group; siRNA: small interfering RNA; Rab23: Rab23, member RAS oncogene family.

invasion, and migration of ovarian cancer cells, we measured the expression of Rab23 in five ovarian cancer cell lines (Caov3, OVCAR3, SKOV3, ES-2, and A2780) and 293 T cells. The expression of Rab23 protein in CaoV3 and A2780 cells was higher than in the other cell lines (Fig. 4A). We downregulated *RAB23* expression in CaoV3 and A2780 cells using RNA interference (Fig. 4A), then changes in the proliferation, invasion, and migration of CaoV3 and A2780 were measured by MTT, Transwell and scratch assay. the MTT assay demonstrated that the proliferation capacity of CaoV3 and A2780 cells decreased after *RAB23* downregulation compared with the control group ($P < 0.05$) (Fig. 4B). The Transwell and scratch assays demonstrated that the invasion and migration abilities of CaoV3 and A2780 cells were significantly weakened after inhibition of *RAB23* expression. ($P < 0.05$) (Fig. 4C-D). These results strongly suggest that downregulation of Rab23 can inhibit the malignant biological behaviors of ovarian cancer cells.

3.7. EMT-related molecules are suppressed after RAB23 downregulation

To measure the effects of Rab23 on the EMT, the expression of EMT-related molecules (E-Cadherin, N-Cadherin, MMP2, and MMP9) in CaoV3 and A2780 cells was measured by Western blot and immunocytochemical staining. These results showed that the protein levels of E-Cadherin increased, while expression of N-Cadherin, MMP2, and MMP9 decreased in response to Rab23 downregulation (Fig. 5A). These findings suggest that the process of EMT in ovarian cancer cells can be suppressed by *RAB23* downregulation. Immunocytochemical staining confirmed these results further (Fig. 5B).

3.8. Inhibition of the Shh-Gli1 and PI3K-AKT signaling pathways after Rab23 downregulation

To measure the effects of Rab23 on the Shh signaling pathway, changes in the expression of Shh and Gli1 in CaoV3 and A2780 were detected after inhibition of *RAB23* by Western blot. These results showed that the protein levels of Shh and Gli1 were decreased in both cell lines after *RAB23* downregulation ($P < 0.05$) (Fig. 6A). Our studies suggest that Rab23 positively regulates the Shh signaling pathway, which could be abrogated by Rab23 inhibition. To further explore the effects of Rab23 on the PI3K-AKT signaling pathway, the protein levels of PI3K, *p*-PI3K, AKT, and *p*-AKT were also measured after *RAB23* decreased. Significant decreases in phosphorylated PI3K and AKT were observed ($P < 0.05$) (Fig. 6B). These findings suggest that the PI3K-AKT signaling pathway can also be suppressed by *RAB23* downregulation.

4. Discussion

Ovarian cancer is the most common gynecological malignant tumor worldwide. Due to the lack of distinct clinical symptoms and specific tumor markers in the early stage, most patients are diagnosed at an advanced stage with extensive abdominal dissemination and metastasis (Bast et al., 2009). At present, the level of the tumor marker CA125 is used to clinically monitor the outcomes in patients with ovarian cancer, but its sensitivity and specificity are not ideal. Therefore, it is critical to explore the causes of ovarian cancer and identify useful markers for early diagnosis, prognosis assessment, and targeted therapy.

In recent years, the role of Rab23 as a proto-oncogene has aroused widespread attention. Many studies have shown that Rab23 can promote the invasion and metastasis of malignant tumors, such as pancreatic ductal adenocarcinoma and liver, gastric, and bladder cancer (Cai et al., 2015; Liu et al., 2007; Hou et al., 2008; Jiang et al., 2016), suggesting that Rab23 acts as an oncogene during the development and progression of malignant tumors. However, some studies demonstrated that the expression of Rab23 in malignant follicular thyroid carcinoma is significantly lower than that of benign follicular thyroid adenoma (Denning et al., 2007), further suggesting that Rab23 also has a tumor-suppressing effect. However, the role of Rab23 in ovarian cancer has not been fully clarified. In this study, we found that Rab23 was highly expressed in ovarian cancer tissues, which suggests that Rab23 plays an important role in the occurrence and development of ovarian cancer. In addition, positive expression of Rab23 in ovarian cancer patients was significantly associated with tumors in stages III-IV. High expression of

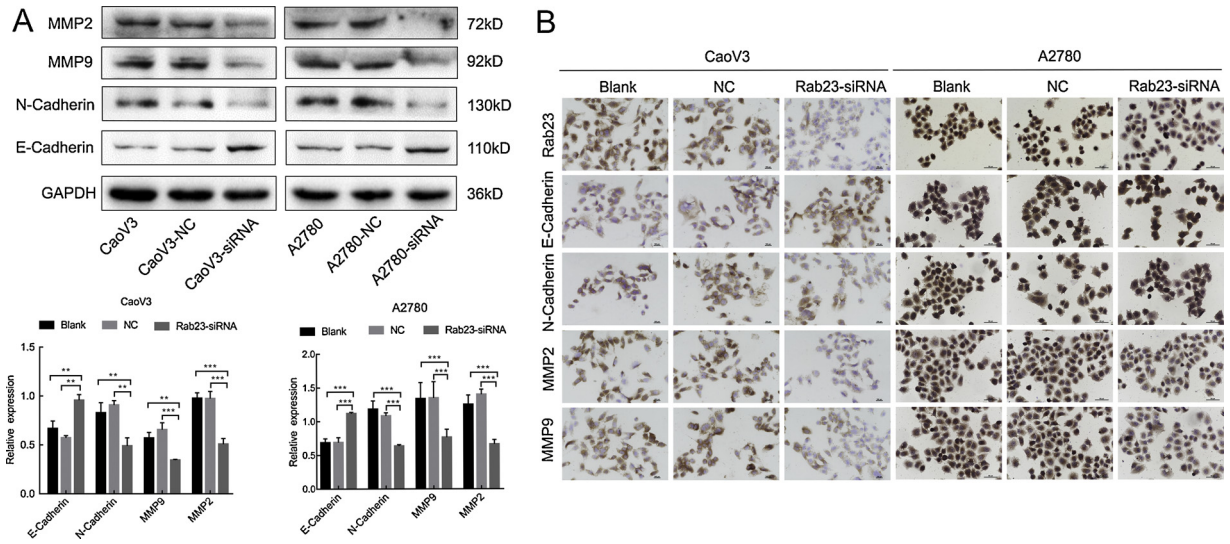

Fig. 5. Effects of Rab23 downregulation on EMT-related proteins in CaoV3 and A2780 cells. (A) Effects of Rab23 downregulation on EMT-related molecules by western blot. (B) Immunocytochemistry staining for EMT-related molecules(E-Cadherin、N-Cadherin、MMP2 and MMP9) in CaoV3 and A2780 after Rab23 downregulation. Scale bar: 100 μm and 50 μm $^{*}P < 0.05$; $^{**}P < 0.01$; $^{***}P < 0.001$. Rab23: Rab23, member RAS oncogene family; Blank: untreated blank control group; NC: negative control group; Rab23-siRNA: downregulated Rab23 expression group; siRNA: small interfering RNA; MMP9: matrix metallopeptidase 9; MMP2: matrix metallopeptidase 2.

Rab23 and stages III-IV were also significantly correlated with poor prognosis. These results further suggest that Rab23 may play an important role in the occurrence and progression of ovarian cancer and may be a potential biomarker to predict prognosis in ovarian cancer patients.

At present, there have been no studies on malignant behaviors and related mechanisms of Rab23 in ovarian cancer except that Rab23 was correlated with platinum drug resistance in ovarian cancer (Zhang et al., 2018). To investigate the effects and mechanisms of Rab23 on the malignant behavior of ovarian cancer cells comprehensively and objectively, we combined datasets from TCGA and DAVID databases to analyze the pathways and functions involving Rab23. The results suggested that the *RAB23* gene was significantly related to the behavior of histone deacetylation, adherent junction, cell proliferation, and the cell cycle. We further confirmed that inhibition of *RAB23* expression decreased the proliferation, migration and invasion capacities of ovarian cancer cells, which was consistent with the results of immunohistochemistry. These results indicated that Rab23 plays a key role in tumor promotion in ovarian cancer.

To further explore the mechanism by which Rab23 affects the

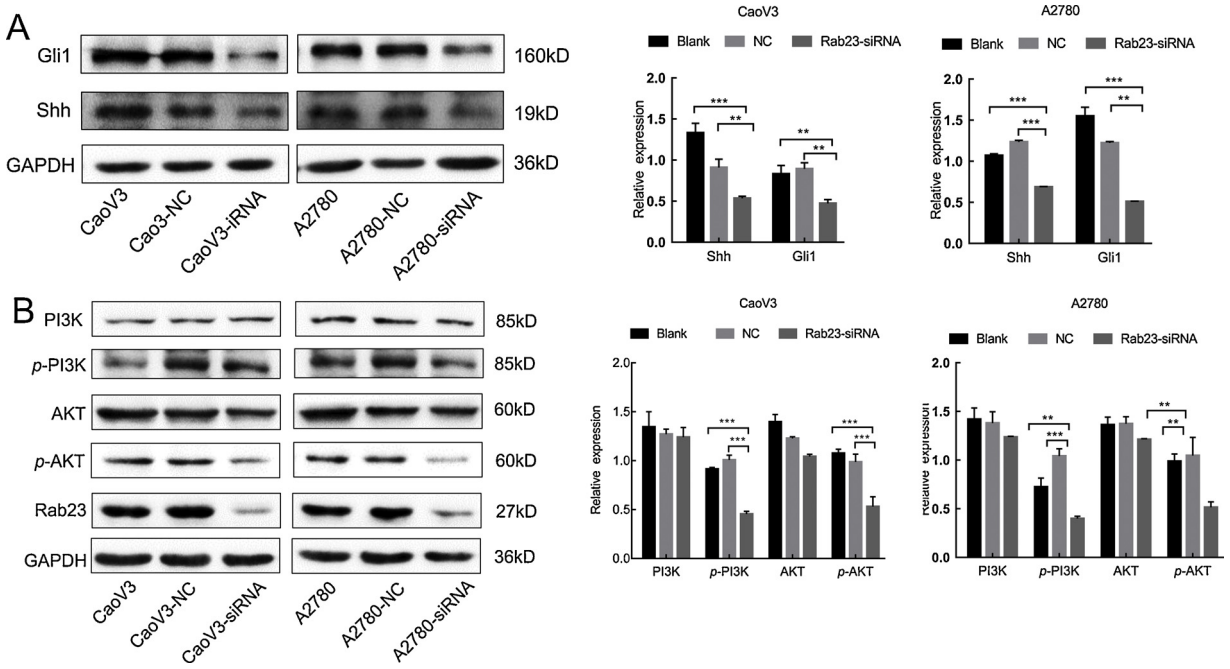

Fig. 6. Effects of Rab23 downregulation on Shh and PI3K-AKT signaling pathways in CaoV3 and A2780 cells. (A) Effects of Rab23 downregulation on the Shh-Gli1 signaling pathway in CaoV3 and A2780 cells detected by western blot. (b) Effects of Rab23 downregulation on PI3K-AKT signaling pathway in CaoV3 and A2780 cells by western blot. $^{*}P < 0.05$; $^{**}P < 0.01$; $^{***}P < 0.001$. Rab23: Rab23, member RAS oncogene family; Blank: untreated blank control group; NC: negative control group; Rab23-siRNA: downregulated Rab23 expression group; siRNA: small interfering RNA; Shh: Sonic Hedgehog; PI3K: phosphoinositide-3-kinase; AKT: AKT serine/threonine kinase; *p*-PI3K: phosphorylation-PI3K; *p*-AKT: phosphorylation-AKT.

malignant behaviors of ovarian cancer cells, we found that the Rab23 was significantly enriched in the Shh signaling pathway in the two databases. Shh signaling plays a critical role in promoting morphogenesis and embryonic development (McMahon et al., 2003), and is also involved in proliferation, invasion, metastasis, and the EMT of malignant tumor cells (Liao et al., 2009). Rab23 plays a different role in regulating the Shh signaling pathway in different malignant tumors. Researchers found that Rab23 overexpression could inhibit the expression of key molecules (Gli1 and Gli2) in the Shh signaling pathway in breast cancer cells (Liu et al., 2015) but not in bladder cancer and squamous cell carcinoma (Jiang et al., 2016; Jian et al., 2016). Our results showed that Shh-Gli1 signaling pathway was significantly inhibited after downregulation of Rab23 protein in ovarian cancer cells, which was consistent with Zhang (Zhang et al., 2018), indicating that there may be differences in the genetic background of different tumors. Alternatively, these results may be due to the intricate interaction between the Shh signaling pathway and other signaling pathways. Indeed, we also found that downregulation of Rab23 could inhibited the EMT process in ovarian cancer, demonstrating that Rab23 may influence the malignant behavior and the EMT process by positively regulating the Shh-Gli1 signaling pathway in ovarian cancer, but the specific mechanism requires further exploration.

The DAVID database also showed that genes in the Rab23 core module were significantly enriched in the pathways involved in cancer. The PI3K-AKT pathway is a tyrosine kinase cascade pathway, which plays an important role in the development and progression of tumors. The abnormal activation of the pathway can promote malignant behaviors in tumor cells, which is also involved in the EMT of various tumors, including ovarian, breast, and gastric cancer (Hu et al., 2016; Lopez-Knowles et al., 2010; Ye et al., 2012). In addition, inhibitors of the PI3K-AKT pathway have been used for targeted therapy against some malignancies (Gasparri et al., 2017). In recent years, inhibitors against the PI3K-AKT signaling pathway have reached the clinical trial stage in ovarian cancer treatment, including both PI3K inhibitors (GDC-09412, BKM120) and AKT inhibitors (perifosine) (Sarker et al., 2015; Matulonis et al., 2017; Hasegawa et al., 2017). Our study demonstrates for the first time that downregulation of *RAB23* can inhibit PI3K-AKT signaling pathway in ovarian cancer cells. Studies have shown that activation of the PI3K-AKT signaling pathway can promote matrix metallopeptidase 9 (MMP9) expression and degrade E-cadherin protein on the surface of tumor cells to further promote tumor invasion and metastasis in head and neck squamous cell carcinoma (Zuo et al., 2011). Thus, we hypothesized that Rab23 could also regulate the expression of MMP9 and MMP2 through the PI3K-AKT signaling pathway, affecting the malignant behavior and EMT in ovarian cancer.

We previously found that the expression of *HE4* correlated with Rab23 protein in ovarian cancer cells by gene chip (Zhu et al., 2016). HE4, also known as orotate protein (WFDC2), is an extracellular secretory protein. In 1999, researchers found that HE4 was highly expressed in ovarian cancer and was approved for clinical detection in 2003 (Hellstrom et al., 2003; Moore et al., 2008, 2009). There have been many clinical reports on HE4, but the mechanism in the occurrence and development of ovarian cancer is still unclear. We previously demonstrated that HE4 could promote the proliferation, invasion, and metastasis of ovarian cancer cells and that Lewis^{y} fucosylation modification of HE4 could further promote the invasion and metastasis of ovarian cancer cells (Zhuang et al., 2014a). We also found that HE4 and ANXA2 could interact with each other and affect the EMT and metastasis through the TGF-β/ERK MAPK signaling pathway in ovarian cancer cells (Zhuang et al., 2014b; Deng et al., 2015). In this study, we found that HE4 can regulate Rab23 expression. Above all, we determined that there is a potential interaction between Rab23 and HE4, although the specific mechanism of the interaction between them needs to be further explored.

In conclusion, we demonstrated that Rab23 is highly expressed in ovarian cancer tissues, and is associated with advanced FIGO stage and poor prognosis. We are the first to report that HE4 can regulate Rab23 expression in ovarian cancer cells. In addition, Rab23 affects the malignant behavior and EMT process by regulating both the Shh and PI3K-AKT signaling pathways. Combined with bioinformatics, these results provide new insights into the pathogenesis, diagnosis, and treatment of ovarian cancer, and provide a new direction for further study of Rab23.

Author's contribution

L. G. and B. L. designed and performed the study. L. G., M. Z., and Q. G. wrote the manuscript. L.G., X. N., X. L., analyzed the data. L. G., J. L., and L. Z. drew the figures. All authors reviewed the manuscript.

Declaration of Competing Interest

The authors declare that there are no conflicts of interest.

Acknowledgments

This work was supported by grants from the National Natural Science Foundation of China (81672590and81472437) and Shengjing Freedom Researchers' plan (201303). The funding body had no role in the design or conduct of the study.

Appendix A. Supplementary data

Supplementary material related to this article can be found, in the online version, at doi:https://doi.org/10.1016/j.biocel.2019.105617.

References

Siegel, R.L., Miller, K.D., Jemal, A., 2017. Cancer Statistics, 2017. CA Cancer J. Clin. 67 (1), 7–30. https://doi.org/10.3322/caac.21387.

Webb, P.M., Jordan, S.J., 2017. Epidemiology of epithelial ovarian cancer. Best Pract. Res. Clin. Obstet. Gynaecol. 41, 3–14. https://doi.org/10.1016/j.bpobgyn.2016.08.006.

Guo, A., Wang, T., Ng, E.L., Aulia, S., Chong, K.H., Teng, F.Y., et al., 2006. Open brain gene product Rab23: expression pattern in the adult mouse brain and functional characterization. J. Neurosci. Res. 83 (6), 1118–1127. https://doi.org/10.1002/jnr.20788.

Olkkonen, V.M., Peterson, J.R., Dupree, P., Lutcke, A., Zerial, M., Simons, K., 1994. Isolation of a mouse cDNA encoding Rab23, a small novel GTPase expressed predominantly in the brain. Gene 138 (1-2), 207–211.

Eggenschwiler, J.T., Espinoza, E., Anderson, K.V., 2001. Rab23 is an essential negative regulator of the mouse Sonic hedgehog signalling pathway. Nature 412 (6843), 194–198. https://doi.org/10.1038/35084089.

Chi, S., Xie, G., Liu, H., Chen, K., Zhang, X., Li, C., Xie, J., 2012. Rab23 negatively regulates Gli1 transcriptional factor in a Su(Fu)-dependent manner. Cell. Signal. 24 (6), 1222–1228. https://doi.org/10.1016/j.cellsig.2012.02.004.

Zhang, W., Yu, F., Wang, Y., Zhang, Y., Meng, L., Chi, Y., 2018. Rab23 promotes the cisplatin resistance of ovarian cancer via the Shh-Gli-ABCG2 signaling pathway. Oncol. Lett. 15 (4), 5155–5160. https://doi.org/10.3892/ol.2018.7949.

Zhu, L., Zhuang, H., Wang, H., Tan, M., Schwab, C.L., Deng, L., et al., 2016. Overexpression of HE4 (human epididymis protein 4) enhances proliferation, invasion and metastasis of ovarian cancer. Oncotarget 7 (1), 729–744. https://doi.org/10.18632/oncotarget.6327.

Bast Jr., R.C., Hennessy, B., Mills, G.B., 2009. The biology of ovarian cancer: new opportunities for translation. Nat. Rev. Cancer 9 (6), 415–428. https://doi.org/10.1038/nrc2644.

Liu, Y.J., Wang, Q., Li, W., Huang, X.H., Zhen, M.C., Huang, S.H., et al., 2007. Rab23 is a potential biological target for treating hepatocellular carcinoma. World J. Gastroenterol. 13 (7), 1010–1017.

Hou, Q., Wu, Y.H., Grabsch, H., Zhu, Y., Leong, S.H., Ganesan, K., et al., 2008. Integrative genomics identifies RAB23 as an invasion mediator gene in diffuse-type gastric cancer. Cancer Res. 68 (12), 4623–4630. https://doi.org/10.1158/0008-5472.can-07-5870.

Jiang, Y., Han, Y., Sun, C., Han, C., Han, N., Zhi, W., Qiao, Q., 2016. Rab23 is overexpressed in human bladder cancer and promotes cancer cell proliferation and invasion. Tumour Biol. 37 (6), 8131–8138. https://doi.org/10.1007/s13277-015-4590-9.

Cai, Z.Z., Xu, L.B., Cai, J.L., Wang, J.S., Zhou, B., Hu, H., 2015. Inactivation of Rab23 inhibits the invasion and motility of pancreatic duct adenocarcinoma. Genet. Mol. Res. 14 (1), 2707–2715. https://doi.org/10.4238/2015.March.30.31.

Denning, K.M., Smyth, P.C., Cahill, S.F., Finn, S.P., Conlon, E., Li, J., et al., 2007. A molecular expression signature distinguishing follicular lesions in thyroid carcinoma using preamplification RT-PCR in archival samples. Mod. Pathol. 20 (10),

1095–1102. https://doi.org/10.1038/modpathol.3800943.
McMahon, A.P., Ingham, P.W., Tabin, C.J., 2003. Developmental roles and clinical significance of hedgehog signaling. Curr. Top. Dev. Biol. 53, 1–114.
Liao, X., Siu, M.K., Au, C.W., Wong, E.S., Chan, H.Y., Ip, P.P., et al., 2009. Aberrant activation of hedgehog signaling pathway in ovarian cancers: effect on prognosis, cell invasion and differentiation. Carcinogenesis 30 (1), 131–140. https://doi.org/10.1093/carcin/bgn230.
Liu, Y., Zeng, C., Bao, N., Zhao, J., Hu, Y., Li, C., Chi, S., 2015. Effect of Rab23 on the proliferation and apoptosis in breast cancer. Oncol. Rep. 34 (4), 1835–1844. https://doi.org/10.3892/or.2015.4152.
Jian, Q., Miao, Y., Tang, L., Huang, M., Yang, Y., Ba, W., et al., 2016. Rab23 promotes squamous cell carcinoma cell migration and invasion via integrin beta1/Rac1 pathway. Oncotarget 7 (5), 5342–5352. https://doi.org/10.18632/oncotarget.6701.
Hu, Z., Cai, M., Deng, L., Zhu, L., Gao, J., Tan, M., et al., 2016. The fucosylated CD147 enhances the autophagy in epithelial ovarian cancer cells. Oncotarget 7 (50), 82921–82932. https://doi.org/10.18632/oncotarget.13289.
Lopez-Knowles, E., O'Toole, S.A., McNeil, C.M., Millar, E.K., Qiu, M.R., Crea, P., et al., 2010. PI3K pathway activation in breast cancer is associated with the basal-like phenotype and cancer-specific mortality. Int. J. Cancer 126 (5), 1121–1131. https://doi.org/10.1002/ijc.24831.
Ye, B., Jiang, L.L., Xu, H.T., Zhou, D.W., Li, Z.S., 2012. Expression of PI3K/AKT pathway in gastric cancer and its blockade suppresses tumor growth and metastasis. Int. J. Immunopathol. Pharmacol. 25 (3), 627–636. https://doi.org/10.1177/039463201202500309.
Gasparri, M.L., Bardhi, E., Ruscito, I., Papadia, A., Farooqi, A.A., Marchetti, C., et al., 2017. PI3K/AKT/mTOR pathway in ovarian Cancer treatment: are we on the right track? Geburtshilfe Frauenheilkd 77 (10), 1095–1103. https://doi.org/10.1055/s-0043-118907.
Sarker, D., Ang, J.E., Baird, R., Kristeleit, R., Shah, K., Moreno, V., et al., 2015. First-in-human phase I study of pictilisib (GDC-0941), a potent pan-class I phosphatidylinositol-3-kinase (PI3K) inhibitor, in patients with advanced solid tumors. Clin. Cancer Res. 21 (1), 77–86. https://doi.org/10.1158/1078-0432.ccr-14-0947.
Matulonis, U.A., Wulf, G.M., Barry, W.T., Birrer, M., Westin, S.N., Farooq, S., et al., 2017. Phase I dose escalation study of the PI3kinase pathway inhibitor BKM120 and the oral poly (ADP ribose) polymerase (PARP) inhibitor olaparib for the treatment of high-grade serous ovarian and breast cancer. Ann. Oncol. 28 (3), 512–518. https://doi.org/10.1093/annonc/mdw672.
Hasegawa, K., Kagabu, M., Mizuno, M., Oda, K., Aoki, D., Mabuchi, S., et al., 2017. Phase II basket trial of perifosine monotherapy for recurrent gynecologic cancer with or without PIK3CA mutations. Invest. New Drugs 35 (6), 800–812. https://doi.org/10.1007/s10637-017-0504-6.
Zuo, J.H., Zhu, W., Li, M.Y., Li, X.H., Yi, H., Zeng, G.Q., et al., 2011. Activation of EGFR promotes squamous carcinoma SCC10A cell migration and invasion via inducing EMT-like phenotype change and MMP-9-mediated degradation of E-cadherin. J. Cell. Biochem. 112 (9), 2508–2517. https://doi.org/10.1002/jcb.23175.
Hellstrom, I., Raycraft, J., Hayden-Ledbetter, M., Ledbetter, J.A., Schummer, M., McIntosh, M., et al., 2003. The HE4 (WFDC2) protein is a biomarker for ovarian carcinoma. Cancer Res. 63 (13), 3695–3700.
Moore, R.G., Brown, A.K., Miller, M.C., Skates, S., Allard, W.J., Verch, T., et al., 2008. The use of multiple novel tumor biomarkers for the detection of ovarian carcinoma in patients with a pelvic mass. Gynecol. Oncol. 108 (2), 402–408. https://doi.org/10.1016/j.ygyno.2007.10.017.
Moore, R.G., McMeekin, D.S., Brown, A.K., DiSilvestro, P., Miller, M.C., Allard, W.J., et al., 2009. A novel multiple marker bioassay utilizing HE4 and CA125 for the prediction of ovarian cancer in patients with a pelvic mass. Gynecol. Oncol. 112 (1), 40–46. https://doi.org/10.1016/j.ygyno.2008.08.031.
Zhuang, H., Hu, Z., Tan, M., Zhu, L., Liu, J., Liu, D., et al., 2014a. Overexpression of Lewis y antigen promotes human epididymis protein 4-mediated invasion and metastasis of ovarian cancer cells. Biochimie 105, 91–98. https://doi.org/10.1016/j.biochi.2014.06.022.
Zhuang, H., Tan, M., Liu, J., Hu, Z., Liu, D., Gao, J., et al., 2014b. Human epididymis protein 4 in association with Annexin II promotes invasion and metastasis of ovarian cancer cells. Mol. Cancer 13, 243. https://doi.org/10.1186/1476-4598-13-243.
Deng, L., Gao, Y., Li, X., Cai, M., Wang, H., Zhuang, H., et al., 2015. Expression and clinical significance of annexin A2 and human epididymis protein 4 in endometrial carcinoma. J. Exp. Clin. Cancer Res. 34, 96. https://doi.org/10.1186/s13046-015-0208-8.